

Modelling the Viscoelastic Response of Anisotropic Materials

J.A. Goshawk and R.S. Jones
Department of Mathematics
University of Wales Aberystwyth
Penglais, Aberystwyth
Dyfed SY23 3BZ

Abstract

A viscoelastic response can be observed during the processing of highly anisotropic, continuous fibre-reinforced composites. Some constitutive relationships which describe anisotropic materials, include an elastic response via an infinitesimal strain tensor. Such models do not take the 'history' of the fluid into account. By adopting a convected frame of reference approach, a viscoelastic model is derived which describe anisotropic fluids with 'memory'. The response of the models in some simple flows is determined.

1 Introduction

Continuous fibre-reinforced composites are highly anisotropic materials which are used in a many areas including the aerospace industry, automotive engineering, marine technology, the sport and leisure industry and medical technology. In many cases the components take the initial form of a flat laminate which consist of plies that have been consolidated. Each individual ply is composed of fibres set in a resin matrix. The laminate is heated to a temperature at which the resin becomes pliable and then deformed into the required form. The resulting flow regime can be extremely complicated and in certain cases the composite laminates have been observed to exhibit a viscoelastic response.

There exist several constitutive descriptions of anisotropic materials. Some of these mathematical representations include the effect of elasticity through

an infinitesimal strain tensor but such models do not account for the 'history' of the material. The aim of this work is to develop a constitutive equation to represent viscoelastic, anisotropic materials with 'memory'. This is achieved by combining ideas of Spencer [1] with those of Oldroyd [2].

In section 2 the kinematics of a class of materials possessing directional qualities are derived using a convected frame of reference approach and shown to concur with existing descriptions. Subsequently, in section 3, the constitutive equations are stated and finally, the behaviour of the new model in unsteady, start-up shear flow is examined in section 4.

2 Kinematics

Let ξ^i be a co-ordinate system embedded in the material such that each particle has the same co-ordinates for all time. Define the metric $\gamma_{ik}(t)$ such that $ds^2 = \gamma_{ik}d\xi^i d\xi^k$, where ds is the distance between an arbitrary pair of neighbouring particles. If a^i is a unit vector that describes the fibre direction at a point then $\gamma_{ik}a^i a^k = 1$ and for neighbouring particles on a given fibre $\delta\xi^i = a^i \delta s$.

In the embedded convected co-ordinate system

$$\frac{\partial a^i}{\partial t} = -a^i \eta_{pq} a^p a^q, \quad (1)$$

where η_{pq} are components of the rate-of-deformation tensor.

On transforming from the convected frame of reference to a fixed Cartesian frame

$$\eta_{pq} \rightarrow d_{pq} = \frac{1}{2} \left(\frac{\partial v_p}{\partial x_q} + \frac{\partial v_q}{\partial x_p} \right), \quad (2)$$

where \mathbf{x} and \mathbf{v} are the position and velocity vectors in the fixed frame respectively, and the partial time derivative, $\partial/\partial t$, in the convected frame transforms to the contravariant convected derivative, $\vartheta/\vartheta t$, in the fixed frame. On using symmetry eq. (1) can be written in the fixed frame as

$$\frac{\vartheta a_i}{\vartheta t} = -a_i a_l a_m \frac{\partial v_l}{\partial x_m}, \quad (3)$$

that is

$$\frac{\partial a_i}{\partial t} + v_l \frac{\partial a_i}{\partial x_l} - a_l \frac{\partial v_i}{\partial x_l} = -a_i a_l a_m \frac{\partial v_l}{\partial x_m}. \quad (4)$$

For inextensible fibres ds^2 is constant which implies $\vartheta a_i/\vartheta t = 0$ so from eqs. 3 and 4

$$a_i a_m \frac{\partial v_l}{\partial x_m} = 0, \quad (5)$$

which is the usual fibre inextensibility condition and

$$\frac{\partial a_i}{\partial t} + v_l \frac{\partial a_i}{\partial x_l} = a_l \frac{\partial v_i}{\partial x_l}, \quad (6)$$

(cf. Spencer [1]).

3 Constitutive equation

The constitutive equation is written as follows

$$\begin{aligned} \sigma_{ik} &= -p\delta_{ik} + T a_i a_k + \sigma'_{ik} \quad (7) \\ \sigma'_{ik} + \lambda_1 \frac{\vartheta \sigma'_{ik}}{\vartheta t} &= 2\eta_T d_{ik} + 2(\eta_L - \eta_T)(a_i a_m d_{mk} + a_k a_m d_{im}) \\ &\quad + \lambda_2 \frac{\vartheta}{\vartheta t} (2\eta_T d_{ik} + 2(\eta_L - \eta_T)(a_i a_m d_{mk} + a_k a_m d_{im})) \quad (8) \end{aligned}$$

where σ_{ik} and σ'_{ik} are components of the stress and extra stress tensors, δ_{ik} are components of the identity tensor, p is the pressure, T is a tension in the fibres arising from the inextensibility condition, η_L and η_T the longitudinal and transverse viscosities respectively and λ_1 and λ_2 the relaxation and retardation times.

4 Unsteady, start-up shear flow

The problem is set within a Cartesian frame of reference $O(x, y, z)$ oriented as shown in fig. 1. The figure shows a composite laminate positioned between two rigid plates of which the upper one is fixed while a velocity, V , is applied to the lower one.

The velocity field throughout the laminate is assumed to be of the form

$$\mathbf{v} = (u(y, t), 0, w(y, t)), \quad (9)$$

which automatically satisfies the continuity equation $\nabla \cdot \mathbf{v} = 0$. The fibre-orientation vector is assumed to be

$$\mathbf{a} = (\cos \alpha(y, t), 0, \sin \alpha(y, t)), \quad (10)$$

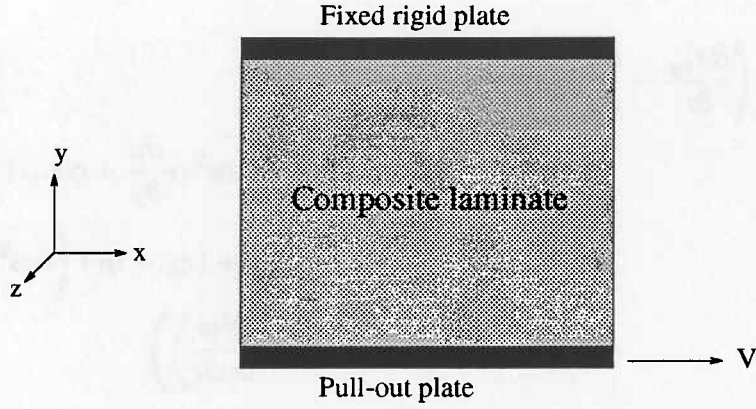


Figure 1: Geometrical configuration for the unsteady, start-up shear flow

so that all the fibres lie within the shear planes. Substituting eqs. (9) and (10) into the fibre inextensibility condition, eq. (5) yields

$$\frac{\partial a_i}{\partial t} = 0, \quad (11)$$

so the fibres do not rotate as the flow progresses.

The equation for the conservation of mass,

$$\rho \frac{D\mathbf{v}}{Dt} = \nabla \cdot \boldsymbol{\sigma} + \rho \mathbf{f}, \quad (12)$$

completes the set of equations required to solve the problem. In eq. (12) ρ denotes the density of the material, D/Dt represents the material derivative and \mathbf{f} is the body force vector. All other quantities are as defined previously.

On substituting the velocity field and fibre-orientation vector into the conservation of mass and constitutive equations they reduce to

$$\rho \frac{\partial u}{\partial t} = \frac{\partial \sigma'_{xy}}{\partial y}, \quad (13)$$

$$\frac{\partial p}{\partial y} = \frac{\partial \sigma'_{yy}}{\partial y}, \quad (14)$$

$$\rho \frac{\partial w}{\partial t} = \frac{\partial \sigma'_{yz}}{\partial y}, \quad (15)$$

and

$$\begin{aligned}
\sigma'_{xy} + \lambda_1 \left(\frac{\partial \sigma'_{xy}}{\partial t} - \frac{\partial u}{\partial y} \sigma'_{yy} \right) &= \eta_T \frac{\partial u}{\partial y} \\
&+ (\eta_L - \eta_T) \left(\cos^2 \alpha \frac{\partial u}{\partial y} + \cos \alpha \sin \alpha \frac{\partial w}{\partial y} \right) \\
&+ \lambda_2 \left(\eta_T \frac{\partial^2 u}{\partial y \partial t} + (\eta_L - \eta_T) \left(\cos^2 \alpha \frac{\partial^2 u}{\partial y \partial t} \right. \right. \\
&\left. \left. + \cos \alpha \sin \alpha \frac{\partial^2 w}{\partial y \partial t} \right) \right) \quad (16)
\end{aligned}$$

$$\begin{aligned}
\sigma'_{yz} + \lambda_1 \left(\frac{\partial \sigma'_{yz}}{\partial t} - \frac{\partial w}{\partial y} \sigma'_{yy} \right) &= \eta_T \frac{\partial w}{\partial y} \\
&+ (\eta_L - \eta_T) \left(\sin^2 \alpha \frac{\partial w}{\partial y} + \cos \alpha \sin \alpha \frac{\partial u}{\partial y} \right) \\
&+ \lambda_2 \left(\eta_T \frac{\partial^2 w}{\partial y \partial t} + (\eta_L - \eta_T) \left(\sin^2 \alpha \frac{\partial^2 w}{\partial y \partial t} \right. \right. \\
&\left. \left. + \cos \alpha \sin \alpha \frac{\partial^2 u}{\partial y \partial t} \right) \right) \quad (17)
\end{aligned}$$

$$\sigma'_{yy} + \lambda_1 \frac{\partial \sigma'_{yy}}{\partial t} = 0, \quad (18)$$

respectively.

These equations are subsequently solved using a numerical time-marching technique.

5 Results

The numerical procedure was tested by simulating the start-up shear flow of a Newtonian fluid. The results were found to agree, to within the tolerance of the numerical scheme, with the textbook analytic solution to the same problem.

The start-up flow of an *inelastic* anisotropic material was then simulated. Fig. 2 shows typical velocity profiles obtained in the x -direction. The fibres were orientated at an angle of 30° to the x -direction through the laminate and the lower rigid plate was displaced with a constant velocity of 0.5 mm/s. As expected the velocity profiles gradually tend towards a steady-state shear flow profile.

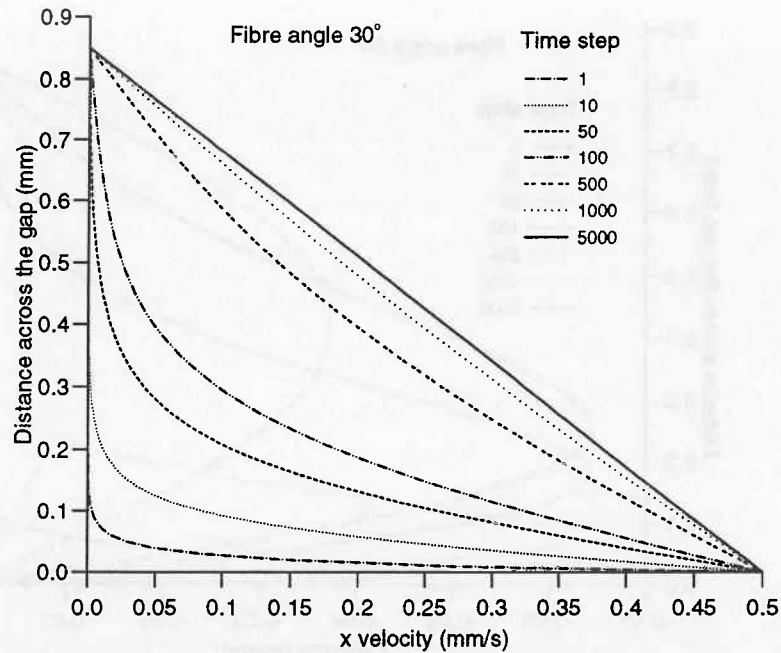


Figure 2: Typical start-up velocities in the x -direction for an inelastic anisotropic fluid

An example of the velocity profiles obtained in the z -direction is given in Fig. 3. It is evident that during the start-up phase of the flow the model predicts a significant velocity in the negative z -direction that decays to zero as steady state is reached.

The effect of elasticity on the velocity field in the x -direction is shown in Fig. 4. In this example the fibres were orientated at an angle of 45° to the x -direction. The relaxation and retardation times are systematically increased with their ratio being kept constant. It is clear that as the elasticity of the material increases it can lead to a large velocity overshoot. In the case where $\lambda_1 = 9 \times 10^{-4}$ s and $\lambda_2 = 1 \times 10^{-4}$ s the velocity within the laminate can be almost twice that of the lower plate. As the simulation progresses in time the expected steady-state profile is obtained for all values of λ_1 and λ_2 .

The velocity field in the z -direction for an elastic anisotropic material is shown in Fig. 5. The figure shows clearly that the velocity in the z -direction is increased significantly by the presence of elasticity. Indeed, for the two most elastic examples shown the material flows in the positive z -direction in some parts of the laminate and the negative z -direction in others.

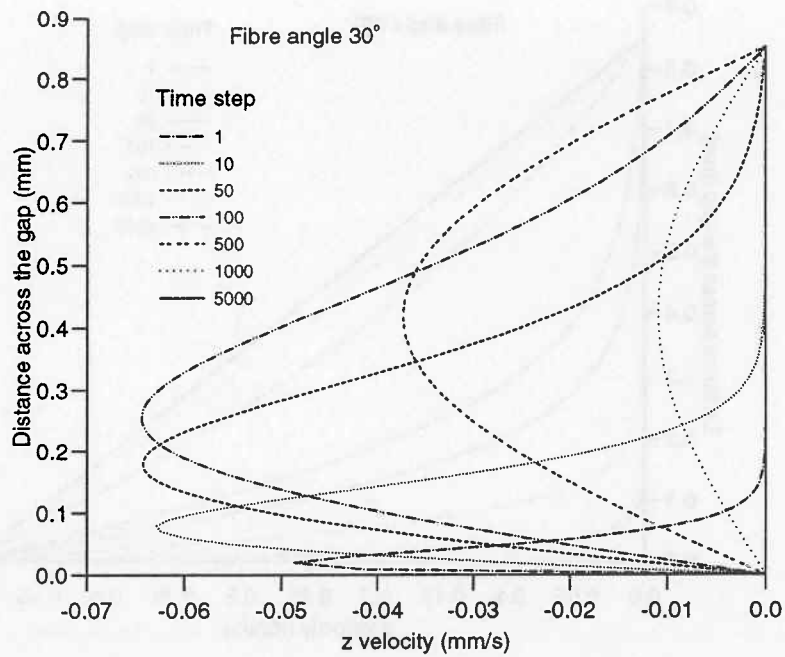


Figure 3: Typical start-up velocities in the z -direction for an inelastic anisotropic fluid

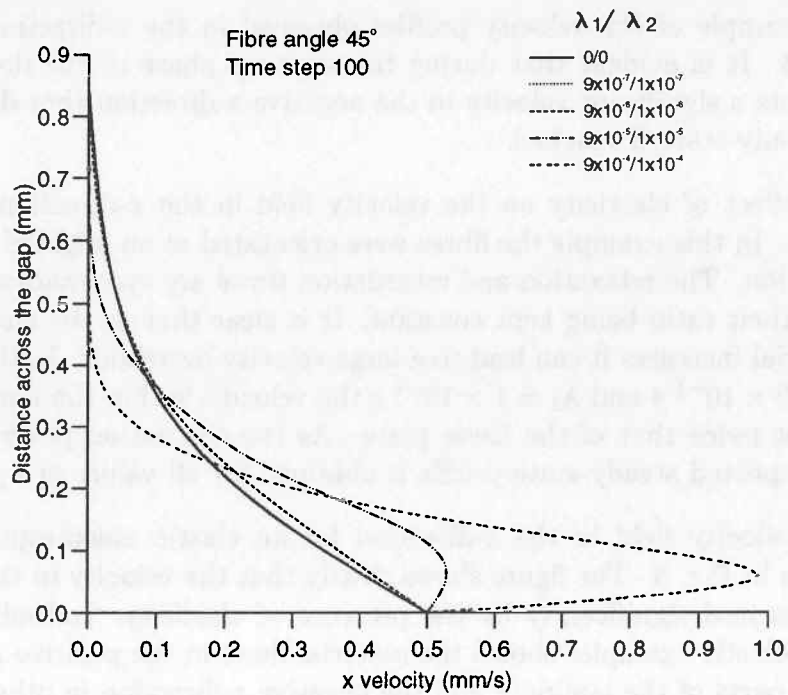


Figure 4: Typical start-up velocities in the x -direction for an elastic anisotropic fluid

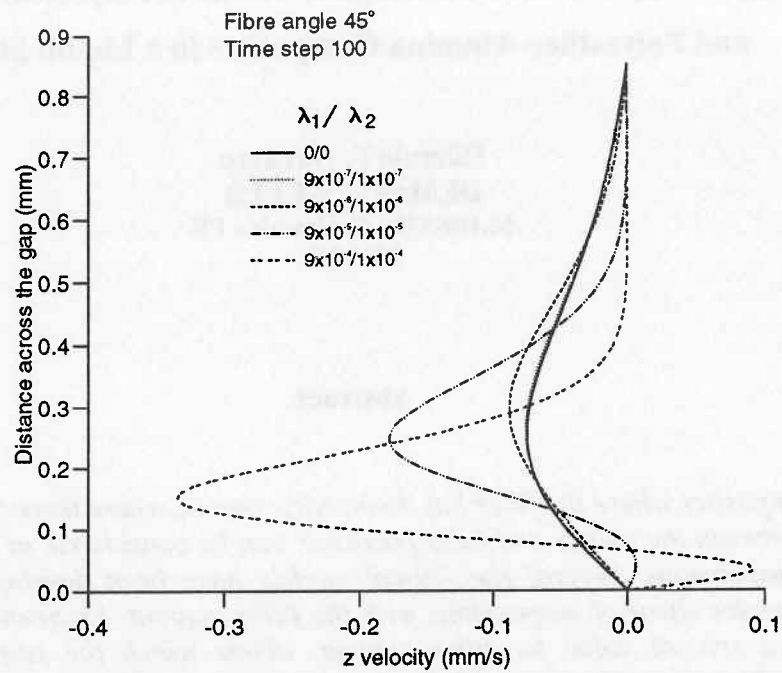


Figure 5: Typical start-up velocities in the z -direction for an elastic anisotropic fluid

References

- [1] Spencer A.J.M., *Deformations of Fibre-reinforced Materials*, (Clarendon Press, Oxford, 1972)
- [2] Oldroyd J.G., *Proc. R. Soc.*, **A245** (1958) 278